

Shear Strengthening Of Reinforced Concrete Beams Using Various CFRP Techniques

Ahmed T. Baraghith¹, Reda N. Behiry^{2*}, and Mahmoud A. Abdel-Aziz²

¹(Associate Professor, Structural Engineering Dept., Faculty of Engineering, Tanta University, Tanta, Egypt)

²(Assistant Professor, Structural Engineering Dept., Faculty of Engineering, Tanta University, Tanta, Egypt)

Abstract:

The utilization of Carbon Fiber Reinforced Polymers (CFRP) has exhibited promising results in enhancing the shear capacity of reinforced concrete (RC) beams. The effectiveness of CFRP is contingent upon its bonding properties with the concrete substrate. The Embedded Through-Section (ETS) technique is distinct from the Externally Bonded (EB) and Near Surface Mounted (NSM) techniques, as the latter two employ CFRP sheets or plates that are attached to the concrete cover of RC beams. The ETS method utilizes CFRP bars that rely on the concrete core of the RC beam. The application of this technique yields a heightened level of confinement, thereby leading to improved bonding efficiency. Furthermore, it can be observed that the ETS technique requires comparatively less concrete preparation in contrast to the EB and NSM techniques. Within this context, an experimental program was implemented to examine the viability of utilizing the ETS technique as a substitute for the EB and NSM techniques to improve the shear strength of twelve concrete beams that exhibited insufficiency in shear. These beams possessed varying shear span-to-depth ratios of 1.50, 2.25, and 3.00. The results suggest that the utilization of the ETS method demonstrates significantly superior efficacy when contrasted with the EB and NSM methods. The specimens reinforced with EB-CFRP sheets, NSM-CFRP plates, and ETS-CFRP bars exhibited an average increase in shear capacity of 30%, 55%, and 83%, respectively, in a comprehensive manner. In addition, it was observed that the ETS method demonstrated a significantly higher level of strengthening efficiency in comparison to the EB and NSM methods, with mean efficiency ratios of 2.8 and 1.4, correspondingly.

Keyword: Shear-deficient beams; Strengthening; Carbon Fiber Reinforced Polymer (CFRP); Embedded Through-Section (ETS); Externally Bonded (EB); Near Surface Mounted (NSM); ETS system's efficiency.

Date of Submission: 09-06-2023

Date of Acceptance: 19-06-2023

I. Introduction

Concrete is the most widely used man-made construction material owing to its high durability and fire resistance [1]. Besides, reinforced concrete (RC) structures are vastly applied in civil engineering structures, including housing and social infrastructure facilities [2-4]. Nevertheless, RC structures require strengthening since such buildings' performance is deteriorated due to several issues (e.g., increased loads due to a change in building use, removal of structural elements due to architectural changes, and calculation errors). Consequently, the strengthening of RC members has arisen as a critical issue for research among structural engineering academics and practitioners [5-7]. Numerous studies have been conducted on the flexural [8-11] and shear [12-15] strengthening of RC beams owing to the fact that an RC beam may possibly collapse under flexural or shear stresses. Shear failure, also known as brittle failure, may occur suddenly and without warning [16,17]. Therefore, the shear failure should be avoided. This has led to the development of a wide variety of strengthening techniques [18-20] that may be used to improve the shear resistance of RC structures. Additional RC or steel components were traditionally used in shear-strengthening deficient RC members. To increase the shear capacity of RC members, it is common practice to (a) add reinforcement around the cross-section and pour concrete around it (also known as a concrete jacket) [21], (b) use fiber reinforced concrete, and (c) mount steel plates on the beam web, also known as a steel jacket [22-24]. Over the past two decades, there has been a growing interest in the field of engineering in the use of fiber reinforced polymer (FRP) for the purpose of improving the capacity of RC elements. Fiber reinforced polymers (FRPs) are made up of a polymer matrix reinforced with continuous fibers often made of carbon (CFRP), glass (GFRP), basalt (BFRP), or aramid (AFRP) [25-27]. FRP offers a variety of benefits as a construction material, including a high tensile strength-to-weight ratio, superior resistance to corrosion and chemicals, ease of handling, and speedy implementation [28-31]. Epoxy external bonding to the substrate concrete surface is a common and widely used technique for utilizing various types of FRP in the process of strengthening RC structures (for example, strips, sheets, and plates) [32-34]. Previous research on the application of externally bonded FRP (EB-FRP) has shown that the efficiency of this technique is dependent on

(a) the quality of the concrete strata, (b) surface preparation, and (c) the bond performance of the concrete-adhesive-FRP interfaces [35,36]. One of the major limitations of the EB method is its thickness, which becomes especially problematic when a large volume of FRP is required. The probability of an unconventional debonding failure is thereby increased [37]. As a result, researchers have spent a considerable amount of time looking for other methods that enable better bonding and a greater degree of interaction between the FRP and the substrate concrete [38,39]. In addition, studies have shown that adding of a mechanical anchor to the end of the FRP may prevent or at least postpone the debonding of the FRP from the concrete, which results in an increase in the member's ability to resist the external loads [40-43].

Another technique for employing FRP, such as strips and bars, to strengthen RC elements is to embed the FRP into the concrete cover. This approach, known as near surface mounted (NSM-FRP), entails placing the FRP into grooves sawed into the concrete cover of the members, polishing and cleaning the grooves, and then filling the grooves with adhesives (epoxy, cement mortar, or grout). As compared to the EB technique, the existing experimental study indicated that the NSM-FRP offers superior composite-concrete bonding and greater confinement produced by the surrounding concrete, which eventually results in greater shear capacity in RC members [44-48]. Nevertheless, the primary drawbacks to this system are the time-consuming surface preparation (groove), the labor-intensive adhesive and FRP installation, the need for sufficient substantial concrete covers, and the limited number of strips or bars that can be inserted due to the need for spacing clearances [49]. Additionally, the predominant failure mechanisms when utilizing the NSM system are concrete fracture followed by debonding of the FRP systems [50]. Hence, debonding of FRP is still unavoidable, and this issue is still the primary drawback of EB- and NSM-FRP methods. The limited tensile strength of the concrete surface constrains the bonding force between the FRP and concrete. Premature debonding of the FRP results in a significant reduction of the maximum strain, which collapses considerably below its ultimate strain. As a consequence, the effectiveness of the FRP strengthening techniques is also reduced [51]. Recent research has proposed an innovative approach for shear strengthening of RC beams called embedded through-section (ETS) [52-58]. During the ETS system's construction, steel or FRP bars are placed into drilled holes in the cross section and then fastened to the concrete substrate using an epoxy resin. As compared to the techniques of externally bonded (EB) and near surface mounted (NSM), the ETS system is easier to install, takes less time, and calls for a less amount of adhesive. Moreover, it does not need any surface preparation or expert laborers. The success of the ETS system, like that of any FRP-based strengthening technique, depends on the bond between the concrete substrate and the embedding bars. This technique also ensures that the embedded bars are confined by the concrete, which enhances bonding characteristics [59-61]. Hence, the ETS system may be a practical and cost-effective alternative when the bonding between the composite and the concrete cover of the element is insufficient to ensure the desired strengthening efficiency for the EB or NSM techniques. Furthermore, the ETS method is appropriate in situations where the concrete cover has corroded or deteriorated to the point where it cannot accommodate other types of FRP strengthening methods, such as EB or NSM.

As presented above, many studies utilized alternative techniques for assessing the shear behavior of RC beams strengthened with FRP (EB, NSM, and ETS). However, to the authors' knowledge, there have been relatively few experimental studies comparing these techniques to one another. So, the purpose of this study is to contribute to a more in-depth knowledge of the behavior of the various CFRP techniques for shear strengthening of RC beams as well as their susceptibility under varied span-to-depth ratios (a/d). In this context, twelve reinforced concrete specimens were fabricated and tested to evaluate the efficiency of various CFRP strengthening techniques with regard to ultimate load capacity, initial stiffness, and energy absorption. A comprehensive description of the experimental program is provided, after which the relevant results are given and discussed.

II. Experimental Program

Test Specimens

The test matrix, as indicated in Table 1, is made up of twelve identical reinforced concrete beams. Shear strengthening technique (EB-CFRP sheets, NSM-CFRP plates, or ETS-CFRP bars) and shear span-to-depth ratio ($a/d = 1.50, 2.25, \text{ or } 3.00$) are the main variables in this study. To facilitate distinguishing between the tested specimens, the letter B_c stands for specimens that haven't been strengthened in any way. While the specimens that have been strengthened with externally bonded CFRP sheets, near surface mounted CFRP plates, or embedded through-section CFRP bars are labeled B_{EB} , B_{NSM} , or B_{ETS} , respectively. The concrete's dimensions and the arrangement of the longitudinal steel reinforcements were the same across the test program. The cross-section was in the shape of a rectangle, measuring 150 millimeters in width and 350 millimeters in total depth; hence, the effective depth (d) was equal to 300 millimeters. The overall center-to-center span of all of the specimens was 2400 mm, whereas the total span of all of the specimens was 2700 mm. The shear span, marked by the symbol a , varied from 450 mm to 900 mm. As a consequence, there were three various shear span-to-depth ratios, which are represented by the symbol's $a/d = 1.50, 2.25, \text{ and } 3.00$, respectively. The reinforcement schemes were designed in accordance with ACI 318-19 [62], with the utilization of a high percentage of longitudinal reinforcement ($\rho_s =$

2.90%) being taken into consideration. This was done because it was anticipated that the test specimens would fail in shear, while the flexural capacity would probably be secured. Each specimen had two layers of steel, the lower layer, tension reinforcement, consisting of four deformed steel bars measuring 22 millimeters in diameter and the upper layer, compression reinforcement, consisting of two bars measuring 16 millimeters in diameter. Each specimen also has a shear defect in one of the two spans. Hence, except for the left side shear span, the stirrups were smooth 8 mm steel bars and spaced every 75 mm as shown in Fig. 1. For reader information's, (1) To ensure that the vertical stirrups did not affect the shear resistance of any of the test specimens, the left-hand shear span was left unreinforced and (2) The effectiveness of the different techniques was also evaluated considering that all strengthening systems (EB-CFRP sheets, NSM-CFRP plates, or ETS-CFRP bars) were quantified in order to provide the same tensile force.

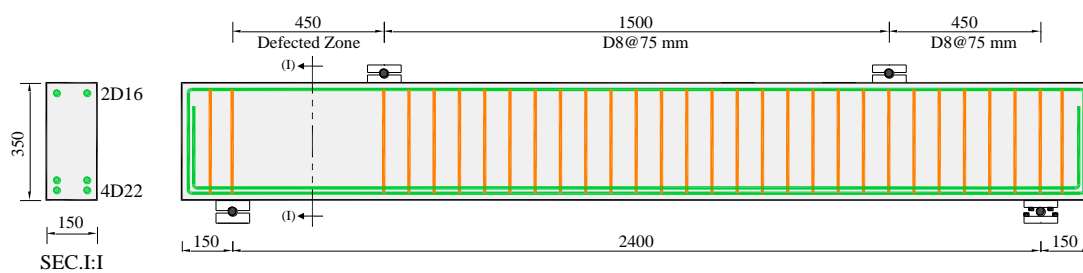
Materials

Concrete

All the test specimens were made using the same identical procedures, starting with casting using ready-mixed concrete in plywood molds and ending with curing using burlap. Crushed limestone with a maximum nominal size of 20 millimeters was used as the coarse aggregate, which had a weight of 1200 kilograms per cubic meter. In addition, there were 800 kilograms per cubic meter of natural sand, 350 kilograms per cubic meter of ordinary Portland cement (OPC type I), and 160 kilograms per cubic meter of water in the mixture. On the day that the specimens were being tested (approximately 28 days later), the concrete's compressive strength was determined by carrying out direct compression tests on cylinder specimens with a diameter of 150 mm and a height of 300 mm in accordance with the ASTM standard [63]. The compressive strengths ranged between 29.7 and 32.4 MPa, with values of 29.7, 30.1, 30.9, 31.5, 31.8, and 32.4. Based on statistics, we can conclude that the mean compressive strength was 31.1 MPa, with a standard deviation of 1.03 MPa and a coefficient of variation of 3.3%.

Table 1 Details of the test matrix.

Strengthening technique	Specimen	Characteristics
Reference	B _{C-1.50}	Control specimen with a/d of 1.50
	B _{C-2.25}	Control specimen with a/d of 2.25
	B _{C-3.00}	Control specimen with a/d of 3.00
Externally Bonded (EB)	B _{EB-1.50}	Strengthened specimen using two plies of EB-CFRP sheets with a/d of 1.50
	B _{EB-2.25}	Strengthened specimen using two plies of EB-CFRP sheets with a/d of 2.25
	B _{EB-3.00}	Strengthened specimen using two plies of EB-CFRP sheets with a/d of 3.00
Near Surface Mounted (NSM)	B _{NSM-1.50}	Strengthened specimen using NSM-CFRP plates with a/d of 1.50
	B _{NSM-2.25}	Strengthened specimen using NSM-CFRP plates with a/d of 2.25
	B _{NSM-3.00}	Strengthened specimen using NSM-CFRP plates with a/d of 3.00
Embedded Through-Section (ETS)	B _{ETS-1.50}	Strengthened specimen using ETS-CFRP bars with a/d of 1.50
	B _{ETS-2.25}	Strengthened specimen using ETS-CFRP bars with a/d of 2.25
	B _{ETS-3.00}	Strengthened specimen using ETS-CFRP bars with a/d of 3.00



(a) Specimens with shear span to depth ratio (a/d) = 1.50

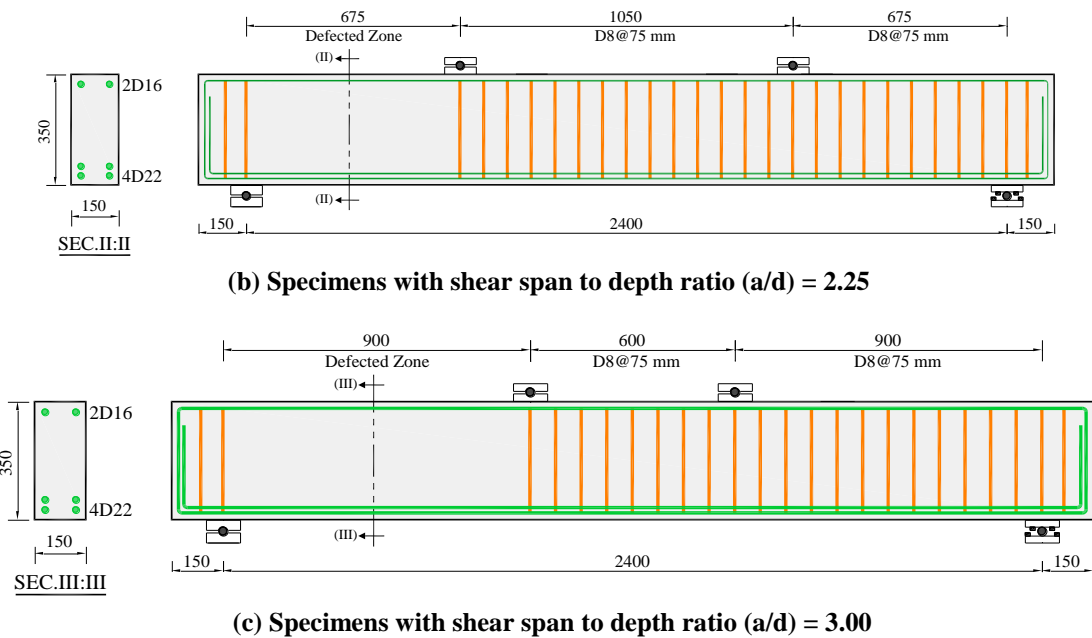


Fig. 1. Geometry and internal steel reinforcements of the tested specimens (All dimensions in mm).

Reinforcing steel

High-strength steel bars with diameters of 22 and 16 millimeters were used for the longitudinal flexural reinforcement of the tested specimens. Nevertheless, for the vertical shear reinforcement, normal-mild steel bars with 8 millimeters in diameter were chosen. Uniaxial tensile tests, conducted per the standards set out by the American Society for Testing and Materials (ASTM) [64], were used to estimate the yield and ultimate tensile strengths. Results showed that steel bars had average yield strengths of 431 ($\epsilon_y = 2155 \mu\epsilon$), 452 ($\epsilon_y = 2260 \mu\epsilon$), and 248 ($\epsilon_y = 1240 \mu\epsilon$) MPa and average ultimate tensile strengths of 605, 619, and 382 MPa for diameters of 22, 16, and 8 millimeters, respectively.

CFRP sheets

As part of the strengthening program, a sheet made of unidirectional carbon fiber reinforced polymer (25 mm width) was used for the externally bonded technique. It was applied continuously across the shear-deficient zone as a U-shaped wrapping around the web. The sheet of carbon fiber reinforced polymer, known commercially as SikaWrap 600C, was adhered to the concrete using an adhesive that is composed of resin and hardener. Both components of the adhesive are specifically designed for structural purposes and provided by the supplier of the CFRP. Table 2 lists the manufacturers' descriptions of the CFRP fabric's mechanical and elastic properties.

CFRP plates

Table 2 details the characteristics of the Sika CarboDur 1214 pultruded plates (20 mm width) used in the near surface mounted technique at room temperature, according to the manufacturer. According to the data shown in this table, the plate has a nominal thickness of 1.20 millimeters. In addition, the tensile strength is 2800 MPa, the modulus of elasticity is 160 GPa, and the ultimate elongation is 1.69%, respectively.

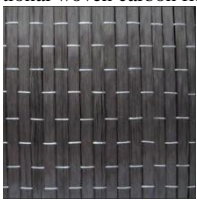


CFRP bars

The technique of strengthening ETS involved the utilization of bars made of carbon fibre reinforced polymer. The aforementioned bars possessed a nominal diameter measuring 8.0 mm and a cross-sectional area of 50.3 mm². The testing approach outlined in ACI 440.3R-04 [65] was employed to determine the tensile strength and modulus of elasticity of the CFRP bars. The tensile strength and modulus of elasticity of the CFRP bars were found to be 2800 MPa and 155 GPa, correspondingly.

Epoxy adhesive

For the different strengthening techniques (EB-CFRP sheets, NSM-CFRP plates, and ETS-CFRP bars), a paste made of epoxy resin that is available for purchase was utilized (Sikadur-330). According to the manufacturer's specifications, its mechanical characteristics are as follows: bond strength of 20.0 MPa, elongation at break of 1.0%, compressive strength of 75.0 MPa, and compressive modulus of 3600 MPa.

Table 2 Mechanical Properties of the used CFRP sheets, plates, and bars.

Type	Description	Nominal Thickness/ Diameter (mm)	Modulus of elasticity (GPa)	Ultimate strength (MPa)	Ultimate elongation (%)
Sheets	Unidirectional woven carbon fiber sheet 	0.33	283	4300	1.80
Plates	Pultruded carbon fiber reinforced polymer plates 	1.20	160	2800	1.69
Bars	Pultruded carbon fiber reinforced polymer bars 	8.0	155	2800	1.80

Strengthening procedure

Externally bonded CFRP (EB-CFRP)

As seen in Figs. 2 through 4, this research makes use of three distinct techniques for shear strengthening concrete beams: externally bonded (EB), near surface mounted (NSM), and embedded through-section (ETS) carbon fiber reinforced polymers. Before the EB-CFRP system was installed, the bonding surface for the EB-CFRP was prepared by: 1) Grinding the concrete with a hand grinder to remove cement laitance, loose, and friable materials; 2) Cleaning the surface with an air compressor to remove dust that would weaken adhesion over time; and 3) Rounding the two corners at the bottom of the web to a minimum radius of 25 mm to prevent stress concentration at the EB-CFRP. Following the manufacturer's instructions [66], resin (A) and hardener (B) were combined in a mixing spindle attached to a slow-speed electric drill (300 rpm) until the mixture became smooth, inconsistent, and evenly gray in color in order to bind the CFRP. The concrete was then coated with a first coat of two-component epoxy resin. Lastly, two plies of CFRP were bonded to the concrete by being impregnated with the same epoxy resin one by one. A roller was utilized to ensure complete saturation and release any trapped air bubbles during the EB-CFRP system's installation.

Near surface embedded (NSM-CFRP)

To efficiently apply the NSM-CFRP strengthening system, it is necessary to carry out the following procedures. The experimental procedure involved the creation of grooves on both lateral sides of the specimen, with dimensions of 15 millimeters in width and 25 millimeters in depth. Then, these grooves were subjected to cleaning using compressed water and air. Subsequently, the grooves were filled with 2/3 of the required volume of epoxy adhesive, which is blended according to the supplier's recommendations. Finally, the CFRP plates were installed into the grooves on both sides of the specimen, and any excess epoxy adhesive was removed.

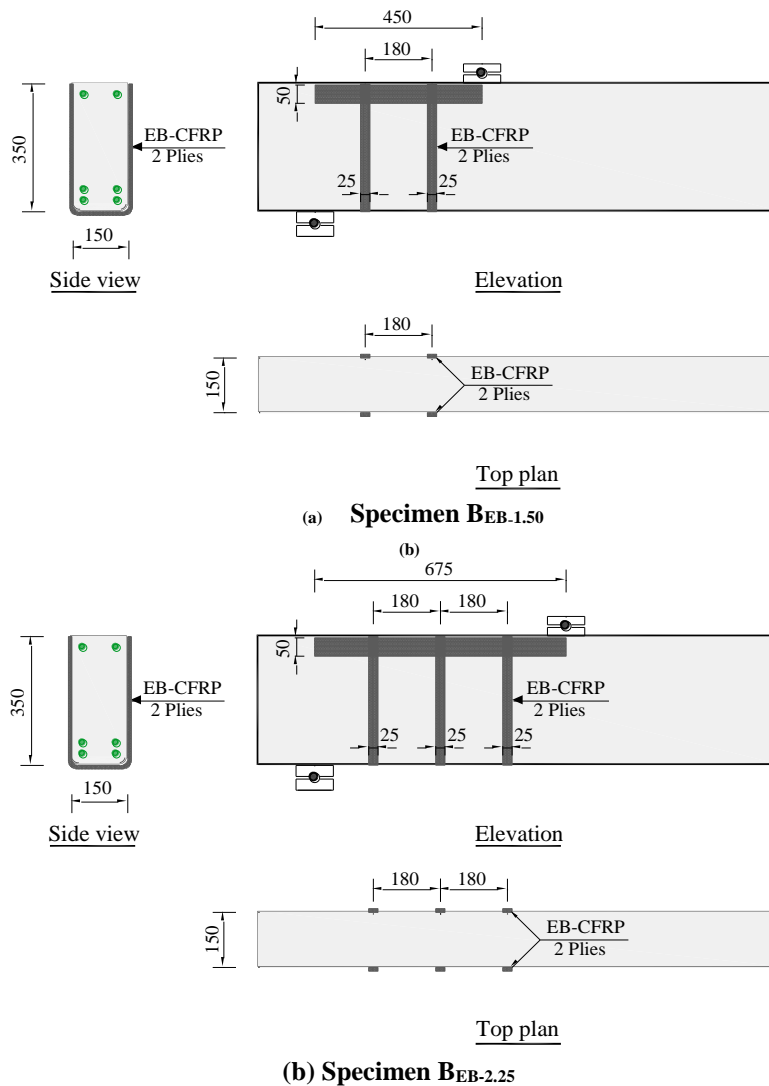
Embedded through-section (ETS-CFRP)

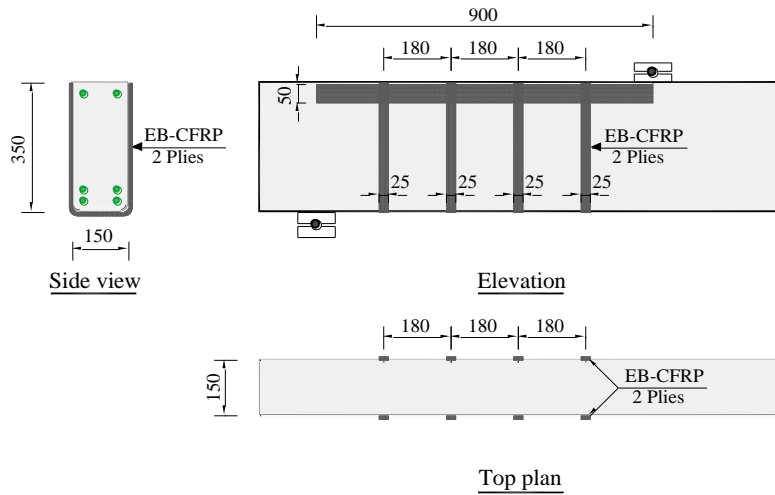
The ETS strengthening procedure consisted of the following activities: (1) The specimen's center was bored with 12-millimeter-diameter holes to accommodate the ETS-CFRP bars. To prevent the adhesive from leaking out of the hole's bottom, its length was determined by leaving 20 mm of concrete cover intact on the specimen's lower side. (2) Particles stuck to the walls of the holes were removed using a helicoidally formed steel brush before being sucked out by a vacuum. (3) The epoxy resin was mixed according to the manufacturer's instructions and poured gently into the holes. (4) The ETS bars were trimmed to size, washed with acetone, and

then carefully inserted into the holes. At least two weeks after the ETS was applied, the specimens were inspected to ensure the adhesive had fully cured.

Test setup and instrumentations

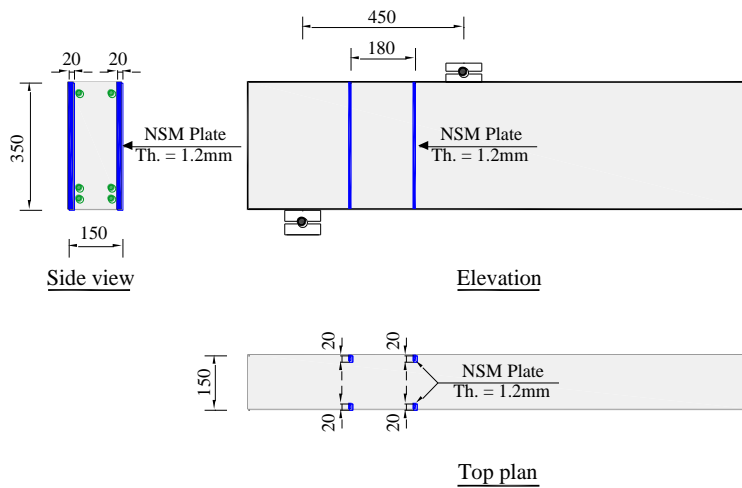
Every specimen was subjected to monotonic loading tests utilizing a four-point loading approach, which is shown in Fig. 5. The applied load was determined with the use of a force transducer with a capacity of 750 kN and an accuracy of 0.1%. To measure the net deflection of the test specimen, four linear variable differential transformers (LVDTs) were set up: two under the span's midpoint and loading point, and two above the supporting points. In addition, two 45-degree LVDTs (Rosette) [67] were installed in the center of the shear span to record the diagonal crack width and associated shear strains. Electrical strain gauges (SGs) were bonded to certain points to find out how much the tension side of internal longitudinal steel, EB-CFRP sheets, NSM-CFRP plates, and ETS-CFRP bars strained. These points were chosen because there is a greater probability that they will give the maximum strain values. In addition, a 100-mm-long Pi-gauge was also used to measure the concrete's compression-side strain. A laser level was used to confirm that the axes of the load cell and the loading test specimens were perpendicular to one another. At each loading step, the vertical mid-span deflection, Pi-gauge readings, main steel strain, and produced tensile strain in the CFRP sheets, plates, and bars were all recorded. The loading rate for each specimen was within the range of 0.1 to 0.2 kN/s. Over the duration of the testing, a data logging device (model number TDS-102) was used in order to capture and save the data.



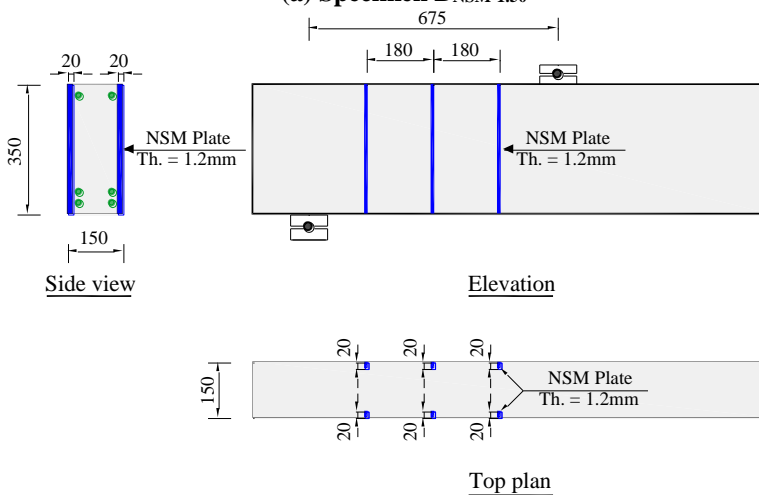


(c) Specimen $B_{EB-3.00}$

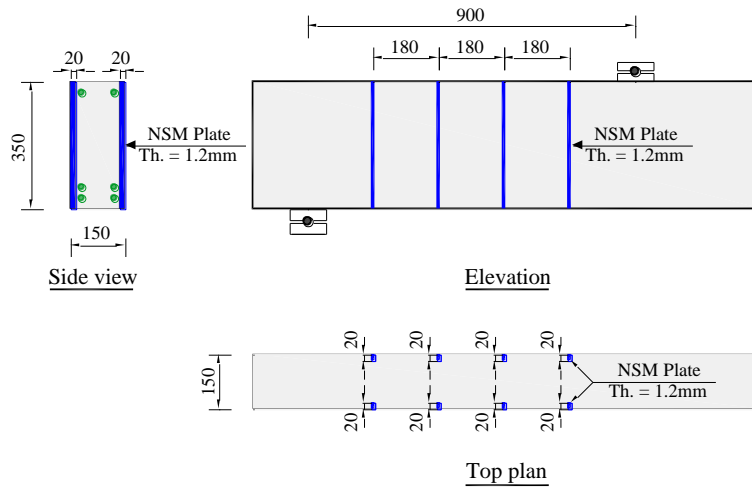
Fig. 2. Scheme of the strengthened specimens using EB-CFRP sheets (All dimensions in mm).



(a) Specimen $B_{NSM-1.50}$

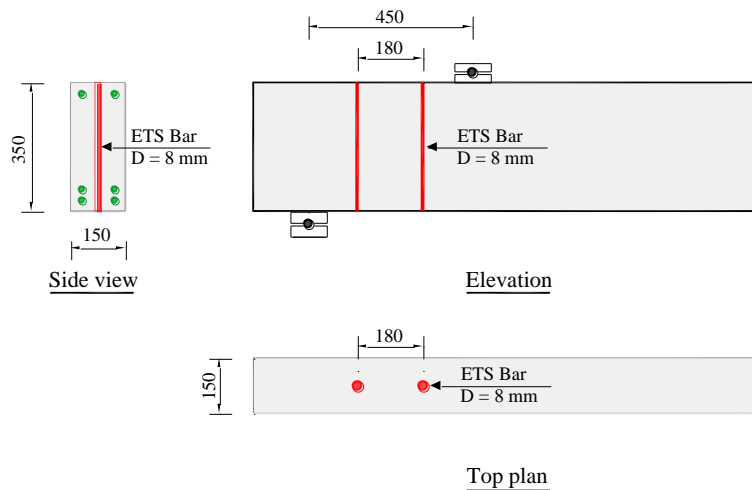


(b) Specimen $B_{NSM-2.25}$

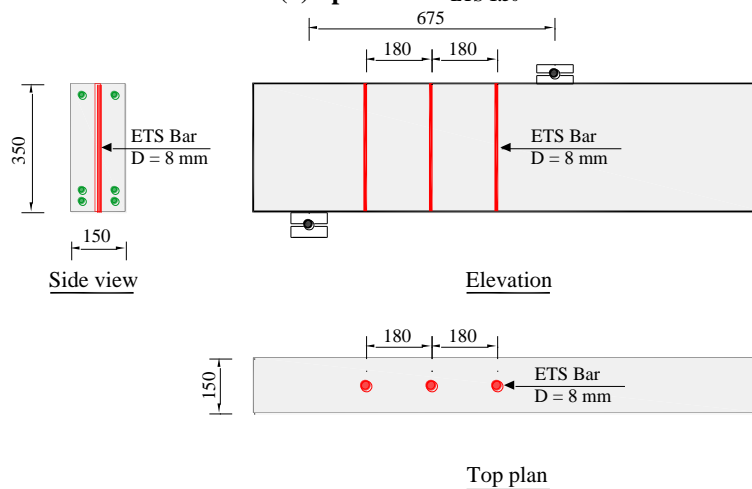


(c) Specimen $B_{NSM-3.00}$

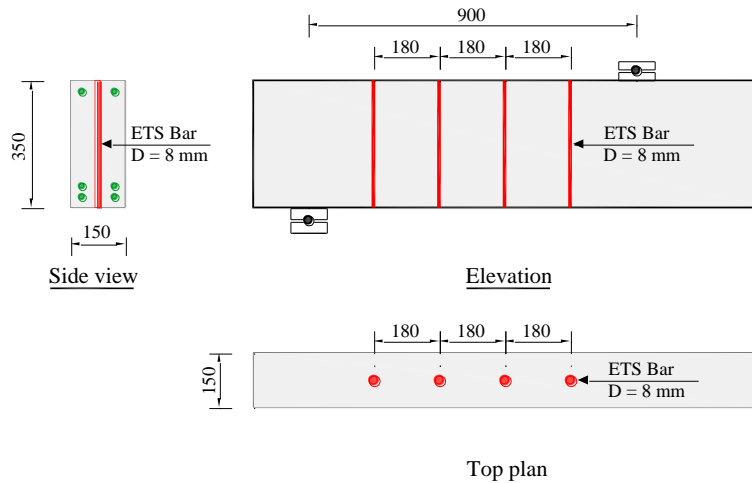
Fig. 3. Scheme of the strengthened specimens using NSM-CFRP plates (All dimensions in mm).



(a) Specimen $B_{ETS-1.50}$



(b) Specimen $B_{ETS-2.25}$



(c) Specimen B_{ETS-3.00}

Fig. 4. Scheme of the strengthened specimens using ETS-CFRP bars (All dimensions in mm).

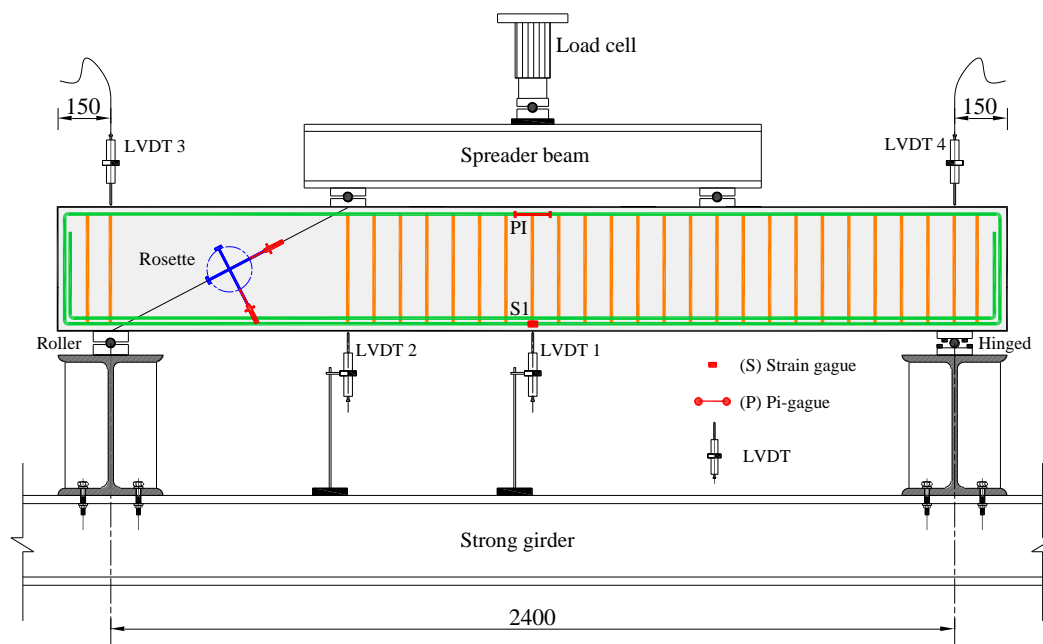


Fig. 5. Test setup and instrumentations (All dimensions in mm).

III. Discussion of Experimental Results

The present section provides a comprehensive evaluation and analysis of the experimental outcomes obtained from all the tested specimens. The primary objective is to compare the effectiveness of various carbon fibre reinforced polymer techniques, namely externally bonded (EB), near surface mounted (NSM), and embedded through-section (ETS), in enhancing the shear resistance of reinforced concrete beams. This comparative analysis encompasses the examination of the crack pattern and failure mode, load carrying capacity, load-deflection response, initial stiffness, energy absorption, and load-strain response. To facilitate the analysis, the experimental outcomes have been separated into three groups based on the shear span-to-depth ratio (a/d).

Crack pattern and failure mode

Figs. 6(a) through 6(c) depict the crack patterns observed in both un-strengthened (reference) and CFRP-strengthened tested specimens. The observed failure mode in the critical shear span of all beams was shear failure, characterized by a diagonal main crack without any flexural yielding of longitudinal reinforcement. The expected mode of failure was observed, as a relatively higher tension reinforcement ratio was implemented to prevent flexural failure. Initially, during the loading process, specimens exhibited flexural cracks in the constant moment

region. The flexural cracking loads were found to be variable based on the a/d values. The results indicate that the flexural cracking load displayed an increasing trend as the a/d ratio decreased. Specifically, specimens with an a/d of 1.50 demonstrated a significantly higher flexural cracking load of approximately 49 kN compared to specimens with a/d of 2.25, which exhibited a load of approximately 32 kN. Moreover, specimens with a/d of 3.00 demonstrated the lowest flexural cracking load of approximately 24 kN. Further loading has caused diagonal shear cracks on the concrete substrate to start at the mid-height of the critical shear span. All techniques employed for strengthening CFRP materials exhibited a delay in the occurrence of the initial shear crack. The first shear cracks in the specimens strengthened with CFRP were observed appearing at higher levels of applied load when compared with the reference beam possessing the same a/d ratio, as indicated in Table 3.

The strengthened specimens with the largest shear span-to-depth ratio ($a/d = 3.00$) exhibited significantly higher shear cracking loads compared to their counterpart specimens with the smallest shear span-to-depth ratio ($a/d = 1.50$). It is noteworthy that specimens strengthened with EB demonstrated a higher cracking load compared to those strengthened with NSM or ETS techniques. The aforementioned observation can be attributed to the superior arrest capabilities of the EB technique to the dominant shear crack located at the central section, as opposed to the NSM and ETS techniques. Finally, the main diagonal shear crack propagated along the diagonal line connecting the loading and support points, and its width progressively increased until the point of failure. The specimens exhibited a consistent pattern of failure based on the shear span-to-depth ratio (a/d). Specifically, a/d values of 1.50 resulted in shear compression failure with crushed concrete in a smaller compression zone oriented parallel to the dominant shear crack, while a/d values of 2.25 and 3.00 led to shear tension failure characterized by diagonal tension perpendicular to the dominant shear crack. In line with the trajectory of the principal tensile stress, the primary shear crack formed at an average inclination of 40° ($a/d = 1.50$) to 27° ($a/d = 3.00$) from the support to the point of load application, as depicted in Fig. 6.

Regarding the CFRP strengthening technique, it was observed that the EB-strengthened specimens ($B_{EB-1.50}$, $B_{EB-2.25}$, and $B_{EB-3.00}$) experienced failure due to debonding of the CFRP sheets, followed by shear compression failure in specimen $B_{EB-1.50}$ or shear tension failure in specimens $B_{EB-2.25}$ and $B_{EB-3.00}$. This failure occurred at the same location as the corresponding reference specimens. During the testing of the NSM-strengthened specimens, namely $B_{NSM-1.50}$, $B_{NSM-2.25}$, and $B_{NSM-3.00}$, an audible popping noise was observed. This noise was a sign on the scratch of the epoxy adhesive that encased the CFRP plates. The final cause of failure was attributed to the splitting of the concrete cover. The NSM-CFRP plates effectively prevented the propagation of shear cracks along the surface of the reinforced concrete beam. Consequently, the NSM-CFRP plates caused the propagation of cracks towards the concrete cover. The final collapse was initiated by the cracking of the concrete cover, leading to the shear failure of the beam.

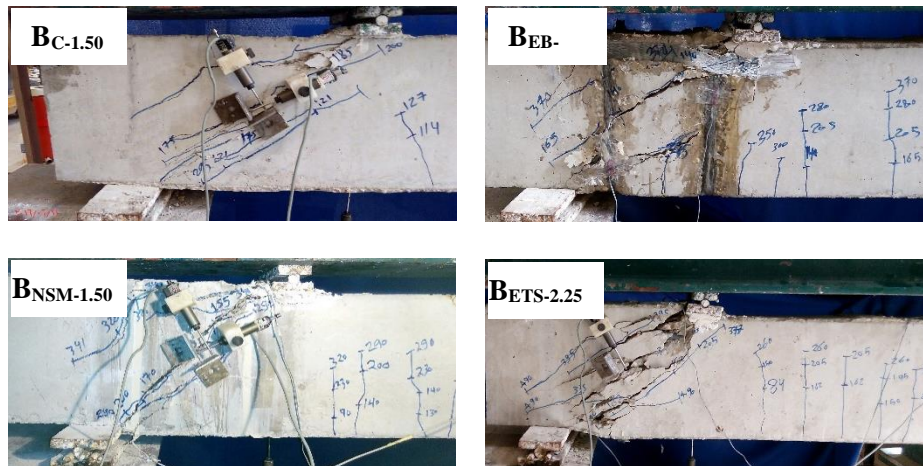
Regarding the ETS shear strengthening system, it has been observed that specimens $B_{ETS-1.50}$, $B_{ETS-2.25}$, and $B_{ETS-3.00}$ have experienced shear failure due to debonding at the interface between the bar and epoxy adhesive. The confinement imposed on ETS bars by the surrounding compressed concrete led to the occurrence of debonding as the predominant failure mode in the bond length of ETS bars that were concentrated in the lower portion of the beam's cross-sectional area. Notwithstanding the aforementioned behaviour, it was observed that the bond performance exhibited the ability to induce significantly higher tensile strains in the CFRP bars in comparison to those achieved through the employment of the EB or NSM techniques, which will be elaborated upon in a later section. The detachment of the concrete cover, which is commonly observed in the NSM technique [68-70], was not observed in the application of the ETS technique.

Ultimate loads

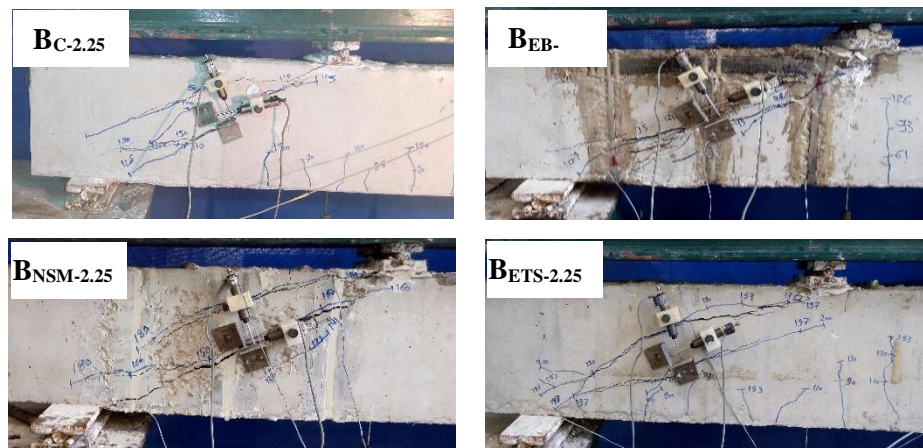
Table 3 provides a brief summary of the ultimate load capacity (P_u) as well as gain in P_u of all specimens that were strengthened with CFRP as compared to their corresponding reference specimens. The tabulated results show that the beams strengthened displayed a significant improvement in their ability to bear loads in comparison to their counterpart un-strengthened specimens, particularly for a greater ratio of shear span-to-depth ($a/d = 3.00$). In details, it was observed that the strengthened specimens with EB-CFRP sheets and NSM-CFRP sheets demonstrated an average rise in their ultimate carrying capacity of approximately 30.0% and 55.0%, respectively, as compared to the corresponding reference specimens. The utilization of the ETS strengthening system, as opposed to the EB and NSM systems, results in a higher ultimate load gain of 82.8%.

The load carrying capacity values emphasized that ETS-CFRP is a more effective method for strengthening RC beams in shear, as evidenced by the higher average gain compared to the other two techniques. Additionally, the cost-effectiveness of ETS-CFRP makes it a viable option for such applications. This statement aligns with the theoretical framework proposed by Mofidi and Chaallal [51] regarding the impact of crack patterns on bond forces. In general, the distribution of cracking on the surface of beams that have been strengthened with FRP is more extensive than that observed in the confined core of the beams. Once the cracks expanded beyond the FRP fibres, the FRP bond length and, as a result, the bond force have been reduced. It follows that debonding happens at a lower force compared with a concrete cross-section with less spread cracking pattern. Hence, the embedded through-section (ETS) technique, which involves the incorporation of fibre reinforced polymer (FRP)

in a concrete core that has fewer cracks, exhibits a lower susceptibility to FRP debonding failure compared to the externally bonded (EB) and near surface mounted (NSM) techniques.



(a) Group (I): $a/d = 1.50$



(b) Group (II): $a/d = 2.25$



(c) Group (III): $a/d = 3.00$

Fig. 6. Failure mode for all tested specimens.

Table 3 Experimental results.

Specimen	Loads (kN)			Deflections (mm)		Stiffness (kN/mm)		Energy absorption (kN.mm)		Maximum strain ($\mu\epsilon$)			Efficiency ratio (ψ_f)		
	P_{cr}	P_u	Capacity* gain %	Δ_{cr}	Δ_u	k_i	Gain* %	E_u	Gain* %	ϵ_s	ϵ_f	ϵ_c	V_f (kN)	V_r (kN)	ψ_f %
Group (I): a/d = 1.50															
BC-1.50	178.3	214.3	--	3.35	3.79	53.2	--	247	--	1068	--	1714	--	--	--
BEB-1.50	192.4	250.5	16.9	3.08	4.47	62.5	17.5	356	44.1	1351	2979	2009	18.1	139.1	13.0
BNSM-1.50	187.1	276.7	29.1	2.84	5.32	65.9	23.9	464	87.9	1481	4495	2110	31.2	131.8	23.7
BETS-1.50	180.9	311.3	45.3	2.41	5.58	75.1	41.2	546	122.1	1653	6409	2393	48.5	138.1	35.1
Group (II): a/d = 2.25															
BC-2.25	118.4	151.0	--	3.59	5.26	33.0	--	234	--	1167	--	1984	--	--	--
BEB-2.25	131.5	193.8	28.3	3.65	5.93	36.0	9.1	363	55.1	1193	3136	2105	21.4	139.1	15.4
BNSM-2.25	127.3	234.2	55.1	3.16	6.68	40.3	22.1	483	106.4	1268	5801	2218	41.6	131.8	31.6
BETS-2.25	121.7	275.2	82.3	2.65	7.06	45.9	39.1	550	135.0	1472	8114	2310	62.1	138.1	45.0
Group (III): a/d = 3.00															
BC-3.00	87.5	111.7	--	3.52	5.30	24.9	--	180	--	1132	--	1863	--	--	--
BEB-3.00	100.2	163.1	46.0	3.77	7.51	26.6	6.8	376	108.9	1213	3930	2006	25.7	139.1	18.5
BNSM-3.00	98.1	202.1	80.9	3.25	8.61	30.2	21.3	544	202.2	1308	6274	2115	45.2	131.8	34.3
BETS-3.00	89.3	246.7	120.9	2.70	9.19	33.1	32.9	656	264.4	1327	9025	2412	67.5	138.1	48.9

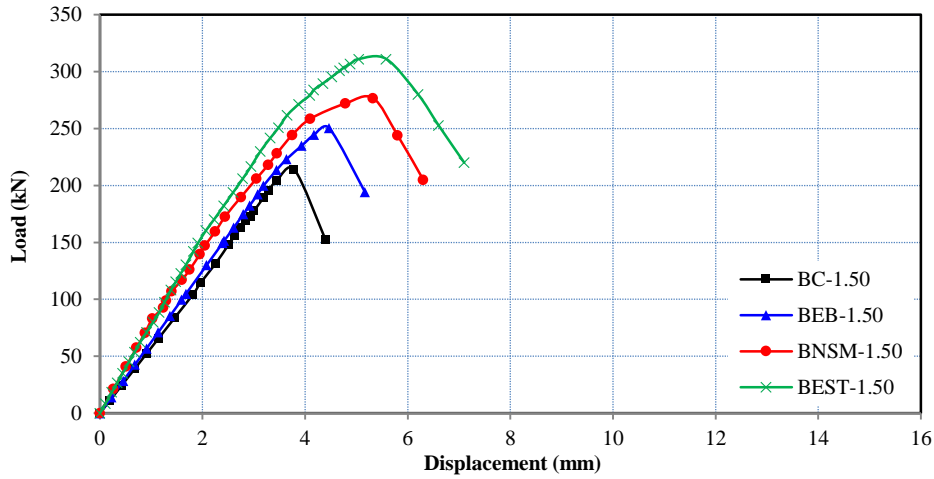
* Calculated relative to their counterpart un-strengthened specimens

P_{cr} = first shear cracking load; P_u = ultimate load; Δ_{cr} = deflection corresponding to the first shear cracking load; Δ_u = deflection corresponding to the P_u ; k_i = initial stiffness; E_u = energy absorption; ϵ_s is the maximum tensile strain of main reinforcement at mid-span section; ϵ_f is the maximum developed tensile strain in the EB-CFRP sheets, NSM-CFRP plates, or ETS-CFRP bars; ϵ_c is the maximum compressive strain in concrete at mid span-section; V_f is the additional capacity provided by the proposed CFRP strengthening techniques; V_r is the rupture tensile strength provided by the proposed CFRP strengthening systems; (ψ_f) is the strengthening's efficiency ratio.

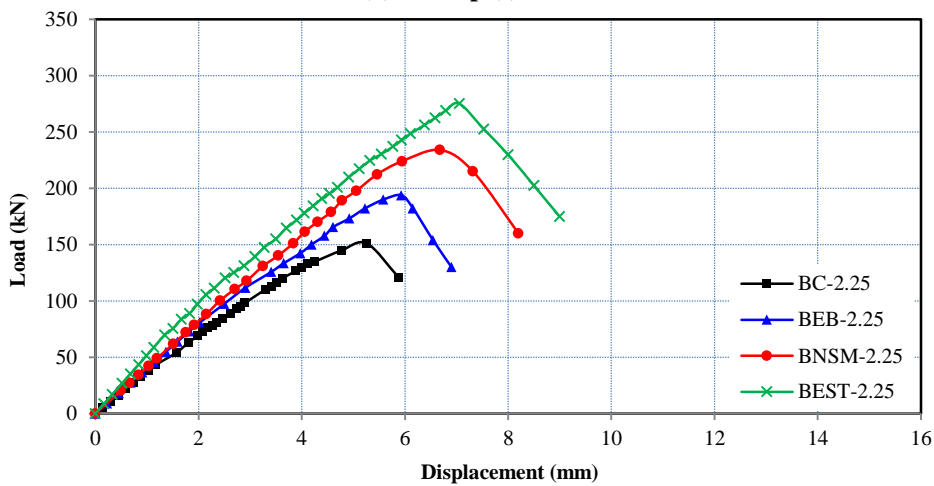
Deformational characteristics

Fig.7 shows the net load-deflection relationships of the reference and strengthened specimens. In general, the three methods of CFRP strengthening techniques (EB, NSM, and ETS) showed considerable improvements over the reference specimens in terms of their responses to deflection, initial stiffness, and energy absorption. Concerning the behavior of deflection, up to the load that causes diagonal cracking, the relationship between the applied load and the net deflection is practically linear for all tested specimens, regardless of whether the specimens have been strengthened or not. In general, deflection increases rapidly and departs from a straight line as the load increases up to failure. Based on the experimental parameters, it is clear that the load-deflection behavior of the reinforced specimens is distinct from that of the reference specimen.

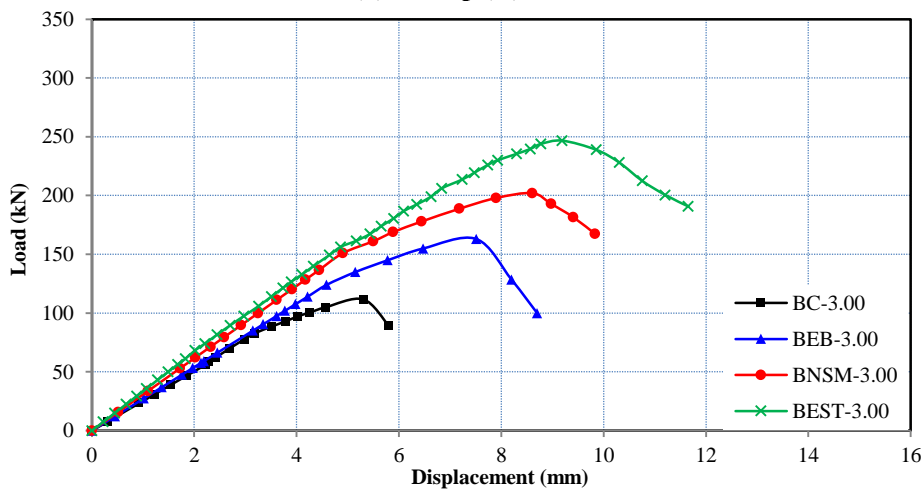
The point at which each specimen's ultimate load was recorded was used to calculate the specimen's displacement capacity, denoted by the symbol Δ_u . This level of displacement would cause the specimen to sustain considerable damage. Table 3 contains a listing of the matching displacement capacity values for each tested specimen. There was a general average increase in displacement capacity (Δ_u) of 24%, 43%, and 52% for strengthened specimens using EB-CFRP sheets, NSM-CFRP plates, and ETS-CFRP bars, respectively, compared to reference specimens. The analysis of the outcomes obtained from the strengthened specimens with varying a/d ratios reveals that the ETS-strengthened specimens exhibited a significantly higher displacement capacity in contrast to the other systems. Specifically, the ETS strengthened specimens provided an increase of 47%, 34%, and 73% for a/d ratios of 1.50, 2.25, and 3.00, respectively, compared to their corresponding un-strengthened specimens.



(a) Group (I): $a/d = 1.50$



(b) Group (II): $a/d = 2.25$



(c) Group (III): $a/d = 3.00$

Fig. 7. Load-deflection responses.

The initial stiffness (k_i) for any specimen has been calculated by utilizing the slope of the load-deflection curve prior to the first diagonal shear crack forming [71]. In respect to the effect of the shear span-to-depth ratio, Table 3 demonstrates that the strengthened specimens had an initial stiffness that was higher than that of the reference specimens. In particular, the strengthened specimens with EB-CFRP sheets and NSM-CFRP plates exhibited an average increase in initial stiffness of 11% and 22%, respectively, compared to the un-strengthened specimens. Utilizing ETS-CFRP bars resulted in an average gain in initial stiffness of 38%, which was notably

higher in comparison to alternative techniques. So, it is suggested that employing ETS may prove to be a more effective approach to enhancing the structural integrity of shear-deficient concrete beams as compared to utilizing EB or NSM systems.

The ductility of strengthened specimens can be evaluated by means of various indicators, one of which is energy absorption (E_u). This indicator is determined by calculating the area under the load-deflection curve from the initial point to the peak point, and it provides information on the ability of the specimens to withstand significant non-elastic deformations prior to failure [72]. In this manner, the specimen $B_{C-3.00}$, which was classified as a reference specimen with a/d ratio of 3.00, exhibited the lowest reported energy absorption value of 180 kN.mm (see Table 3). Whereas the utilization of EB-CFRP sheets, NSM-CFRP plates, and ETS-CFRP bars for strengthening this specimen ($B_{C-3.00}$) resulted in a significant enhancement in energy absorption, with increments of approximately 109%, 202%, and 264%, respectively. The energy absorption capacities of the EB-strengthened specimens with $a/d = 1.50, 2.25,$ and 3.00 were compared to their counterpart ETS-strengthened specimens, and it was found that the energy absorption capacities of ETS-strengthened specimens were 1.53, 1.52, and 1.74 times greater than EB-strengthened specimens, respectively. With respect to the strengthened specimens $B_{NSM-1.50}, B_{NSM-2.25},$ and $B_{NSM-3.00}$, it was observed that the ETS-strengthened specimens $B_{ETS-1.50}, B_{ETS-2.25},$ and $B_{ETS-3.00}$ exhibited the ability to absorb 1.18, 1.14, and 1.21 times more energy, respectively. Overall, it was evident that using the ETS technique as a strengthening system resulted in a superior improvement in the ductility behavior when compared to EB or NSM systems.

Strain response

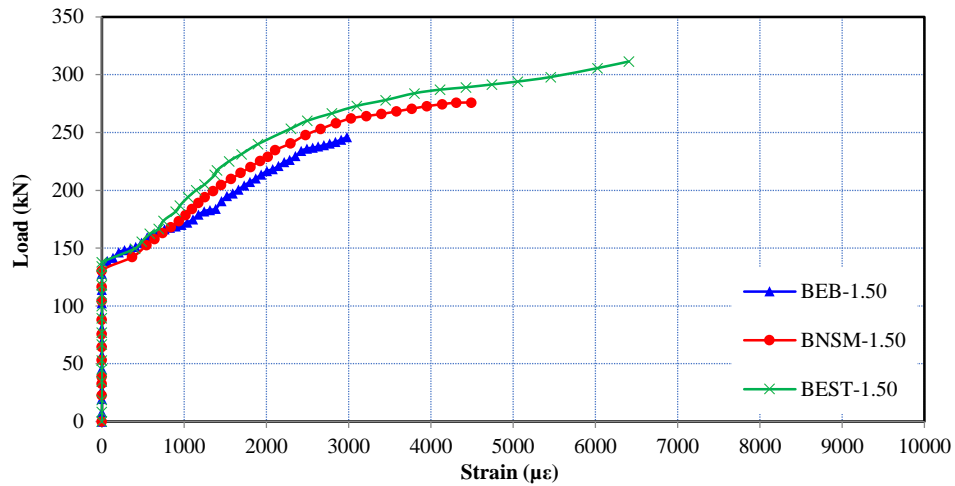
As outlined in the section pertaining to test setup and instrumentations, a comprehensive arrangement of instruments was meticulously designed to facilitate the monitoring of strain, thereby enabling the acquisition of crucial information and data requisite for comprehending the mechanism of shear resistance involved in the strengthened specimens, which were subjected to diverse CFRP strengthening systems. Strain gauges were employed to quantify various strains, including the compressive strain of concrete, the tensile strain of flexural reinforcement, and the tensile strains of the EB-CFRP sheets, NSM-CFRP plates, and ETS-CFRP bars. In cases where an electric strain gauge exhibited irregular behaviour suggestive of reinforcement debonding before the specimen's failure, the corresponding data points were excluded.

Compressive and tensile flexural strains

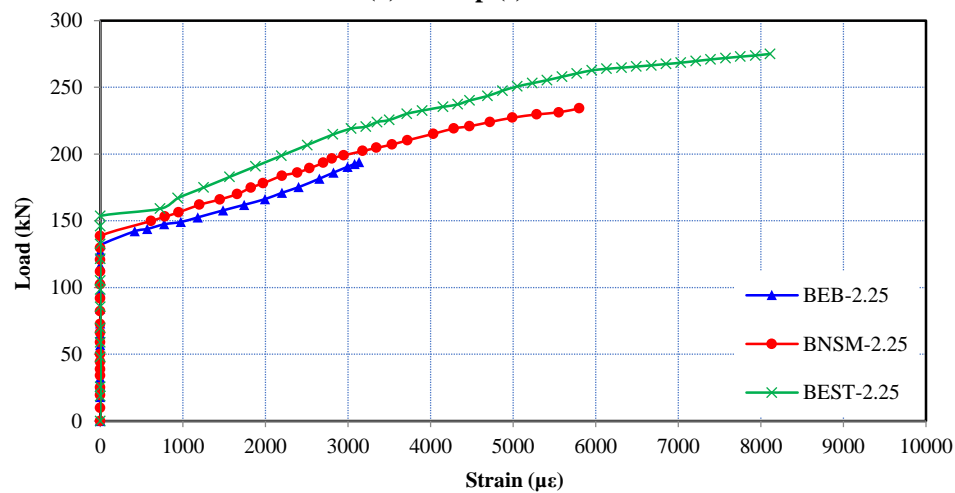
Table 3 presents the outcomes of the maximum compressive strain observed in the tested specimens. The $B_{ETS-1.50}$ exhibited the highest value ($\epsilon_{cmax} = 2393 \mu\epsilon$); however, it did not attain the maximum compression strain in flexure ($\epsilon_{cu} = 3000 \mu\epsilon$) as prescribed by ACI 318-19 [62]. This ensured that the failure modes of the specimens were controlled by shear rather than flexural failure. Furthermore, the findings of the strain analysis demonstrate the efficiency of the proposed strengthening techniques. To clarify, the strengthened specimens exhibited maximum tensile strains of flexural reinforcement at failure that were approximately 1.20 times greater than those observed in the un-strengthened specimens. The aforementioned observation suggests that the proposed strengthening techniques exhibited superior performance in terms of postponing the failure of the non-ductile shear by enabling the flexural steel to move closer to the yield region by one step.

CFRP strains

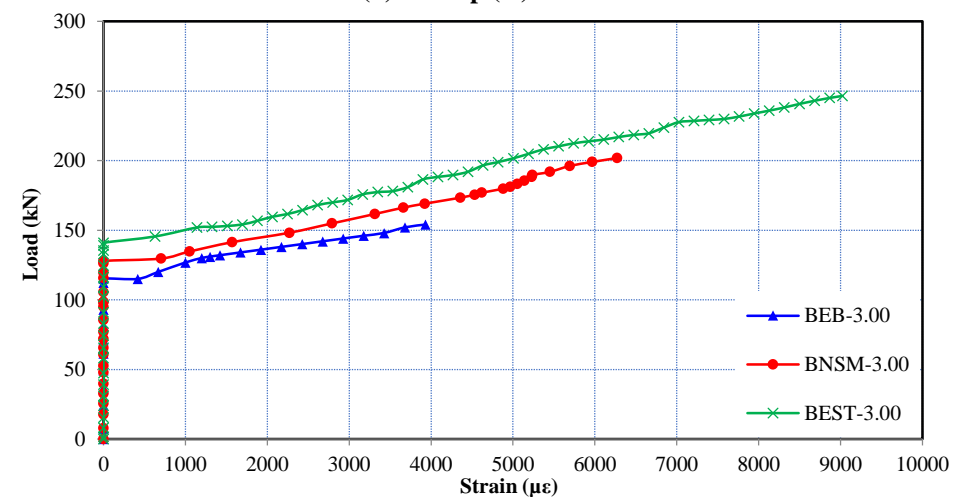
The load-CFRP strain relationship observed in the strengthened specimens of EB-CFRP sheets, NSM-CFRP plates, and ETS-CFRP bars displayed a bi-linear pattern, as depicted in Fig. 8. The initial stage of the load-strain relationship is depicted by a line originating from the point of origin and extending along the vertical axis until the appearance of the first diagonal shear crack. This phenomenon indicates that the strengthening systems did not initially contribute to the shear capacity prior to the formation of the initial crack. After the propagation of the cracks, the second phase was initiated by an abrupt increase in the strains, which continued until the point of failure. The strain of CFRP exhibits a rising trend with the increase in the applied load until it reaches a specific level, depending on the method of strengthening. For example, strengthened specimens $B_{EB-1.50}, B_{NSM-1.50},$ and $B_{ETS-1.50}$ achieved maximum CFRP strains of 2979 $\mu\epsilon, 4495 \mu\epsilon,$ and 6409 $\mu\epsilon$, respectively. It is noteworthy to state that an increase in the shear span-to-depth ratio (a/d) results in a higher degree of strain development in the strengthening system. The reversal of the curves depicted in Fig. 8 is indicative of the preference for the ETS system over alternative systems for the purpose of shear strengthening of reinforced concrete beams.



(a) Group (I): $a/d = 1.50$



(b) Group (II): $a/d = 2.25$



(c) Group (III): $a/d = 3.00$

Fig. 8. Load-CFRP strain responses.

The ETS system's efficiency

The strengthened specimens exhibited greater shear capacities compared to the reference specimens, despite the fact that the CFRP system did not attain its maximum tensile strength. This was due to the predominant failure mode being debonding. So, in order to assess the efficiency of the strengthening technique, the CFRP efficiency ratio (ψ_f) was computed for every strengthened specimen and is listed in Table 3. The efficiency ratio can be mathematically expressed as the ratio of the shear resistance contribution of carbon fiber reinforced

polymers (V_f) to their rupture tensile strength (V_r). The shear capacity of a strengthened specimen can be determined using the principle of simple superposition, which involves the summation of two distinct contributions. These contributions include the shear capacity provided by the concrete (V_c) and the additional capacity provided by the proposed CFRP strengthening systems (V_f). Thus, the contribution of the CFRP strengthening system ($V_f = V_u - V_c$) may be evaluated experimentally as the difference in ultimate shear load (V_u) between a strengthened specimen and the reference specimen. Table 3 displays the efficiency of the three types of CFRP strengthening techniques for every specimen. The results indicate that the ETS-CFRP exhibits superior efficiency compared to the EB-CFRP and NSM-CFRP techniques, with average ratios of 2.8 and 1.4 for all shear span-to-depth ratios, respectively. This suggests that the ETS-CFRP strengthening techniques exhibit a higher degree of cost-effectiveness in comparison to alternative methods.

IV. Summary and Conclusion

The purpose of this study is to report the results of a research investigation that examines the efficiency of the Embedded Through-Section (ETS) technique in comparison to alternative techniques, namely Externally Bonded (EB) and Near Surface Mounted (NSM). Based on the discussions presented in the current study, the following conclusions have been derived:

- The utilization of different CFRP strengthening techniques, specifically ETS, has the potential to significantly improve the shear capacity of reinforced concrete beams, even in cases where transverse steel reinforcement is not present. The results indicate that the beam strengthened with EB-CFRP sheets, NSM-CFRP plates, and ETS-CFRP bars exhibited an average increase in shear capacity of 30%, 55%, and 83%, respectively.
- The comparative analysis of the shear strengthening effectiveness achieved through the use of externally bonded (EB) and near surface mounted (NSM) techniques with that of embedded through-section (ETS) revealed that the latter is more efficacious. The relatively high maximum tensile strain of CFRP bars was achieved, particularly with $a/d = 3.00$, owing to the favorable confinement introduced by the concrete core of the beams, which ensured good bond conditions of ETS bars.
- The ETS technique outperformed the FRP-based EB and NSM shear strengthening techniques across all shear span-to-depth ratios. The ETS technique demonstrated a significantly higher level of strengthening efficiency compared to the EB and NSM techniques, with respective efficiency ratios of 2.8 and 1.4, on average.
- The energy absorption capacity of specimens strengthened with ETS-CFRP bars was found to be significantly higher than those strengthened with EB-CFRP sheets and NSM-CFRP plates. The magnitude of this increase was notably greater in the reinforced specimens featuring a high ratio of shear span-to-depth. Regarding the ratio of a/d being 3.00, it was noted that ETS strengthened specimens demonstrated a higher capacity to absorb energy, with an increase of 1.7 and 1.2 times compared to the specimens strengthened with EB or NSM, respectively.
- Based on the results of the conducted experimental program, which showed a significant increase in shear strengthening effectiveness at $a/d = 1.50$, it can be concluded that the use of ETS can effectively prevent brittle failure in reinforced concrete beams that are susceptible to sudden debonding of either EB or NSM systems, and instead promote a ductile shear failure mode. In addition, the ETS method presents a cost-effective and environmentally sustainable approach for shear strengthening. As it exhibits a lower susceptibility to the adverse impact of elevated temperatures compared to the utilization of external systems.

References

- [1]. Neville, A.M. and Brooks, J.J., 1987. Concrete technology (Vol. 438). England: Longman Scientific & Technical.
- [2]. Huang, B.T., Dai, J.G., Weng, K.F., Zhu, J.X. and Shah, S.P., 2021. Flexural performance of UHPC–concrete–ECC composite member reinforced with perforated steel plates. *Journal of Structural Engineering*, 147(6), p.04021065. [https://doi.org/10.1061/\(asce\)st.1943-541x.0003034](https://doi.org/10.1061/(asce)st.1943-541x.0003034).
- [3]. Li, S., Chan, T.M. and Young, B., 2022. Mechanical analysis and finite element modeling of FRP-ECC-HSC composite stub column under axial compression. *Journal of Building Engineering*, 62, p.105212. <https://doi.org/10.1016/j.jobbe.2022.105212>.
- [4]. Yin, X., Li, Q., Xu, X., Chen, B., Guo, K. and Xu, S., 2023. Investigation of continuous surface cap model (CSCM) for numerical simulation of strain-hardening fibre-reinforced cementitious composites against low-velocity impacts. *Composite Structures*, 304, p.116424. <https://doi.org/10.1016/j.compstruct.2022.116424>.
- [5]. Teng, J.G., Chen, J.F., Smith, S.T. and Lam, L., 2002. FRP: strengthened RC structures (p. 266).
- [6]. Smith, S.T. and Teng, J.G., 2002. FRP-strengthened RC beams. I: review of debonding strength models. *Engineering structures*, 24(4), pp.385-395. [https://doi.org/10.1016/s0141-0296\(01\)00105-5](https://doi.org/10.1016/s0141-0296(01)00105-5).
- [7]. Su, M.N., Wei, L., Zhu, J.H., Ueda, T., Guo, G.P. and Xing, F., 2019. Combined impressed current cathodic protection and FRCM strengthening for corrosion-prone concrete structures. *Journal of Composites for Construction*, 23(4), p.04019021. [https://doi.org/10.1061/\(asce\)cc.1943-5614.0000949](https://doi.org/10.1061/(asce)cc.1943-5614.0000949).
- [8]. Yang, X., Gao, W.Y., Dai, J.G., Lu, Z.D. and Yu, K.Q., 2018. Flexural strengthening of RC beams with CFRP grid-reinforced ECC matrix. *Composite Structures*, 189, pp.9-26. <https://doi.org/10.1016/j.compstruct.2018.01.048>.
- [9]. Huang, B.T., Li, Q.H., Xu, S.L. and Zhang, L., 2019. Static and fatigue performance of reinforced concrete beam strengthened with strain-hardening fiber-reinforced cementitious composite. *Engineering Structures*, 199, p.109576. <https://doi.org/10.1016/j.engstruct.2019.109576>.

- [10]. Huang, B.T., Li, Q.H., Xu, S.L. and Zhou, B., 2019. Strengthening of reinforced concrete structure using sprayable fiber-reinforced cementitious composites with high ductility. *Composite Structures*, 220, pp.940-952. <https://doi.org/10.1016/j.compstruct.2019.04.061>.
- [11]. Li, Q., Yin, X., Huang, B., Zhang, Y. and Xu, S., 2022. Strengthening of the concrete face slabs of dams using sprayable strain-hardening fiber-reinforced cementitious composites. *Frontiers of Structural and Civil Engineering*, 16(2), pp.145-160. <https://doi.org/10.1007/s11709-022-0806-4>.
- [12]. Baraghith, A.T., Mansour, W., Behiry, R.N. and Fayed, S., 2022. Effectiveness of SHCC strips reinforced with glass fiber textile mesh layers for shear strengthening of RC beams: Experimental and numerical assessments. *Constr Build Mater*, 327, p.127036. <https://doi.org/10.1016/j.conbuildmat.2022.127036>.
- [13]. Baraghith, A.T., Khalil, A.H.A., Etman, E.E. and Behiry, R.N., 2023, April. Improving the shear behavior of RC dapped-end beams using precast strain-hardening cementitious composite (P-SHCC) plates. In *Structures* (Vol. 50, pp. 978-997). <https://doi.org/10.1016/j.istruc.2023.02.059>.
- [14]. Younis, A., Ebead, U. and Shrestha, K.C., 2017. Different FRCM systems for shear-strengthening of reinforced concrete beams. *Construction and Building Materials*, 153, pp.514-526. <https://doi.org/10.1016/j.conbuildmat.2017.07.132>.
- [15]. Khalil, A.E.H.A., Atta, A.M., Baraghith, A.T., Behiry, R.N. and Soliman, O.E., 2023. Shear strengthening of concrete deep beams using pre-fabricated strain-hardening cementitious composite plates. *Engineering Structures*, 278, p.115548. <https://doi.org/10.1016/j.engstruct.2022.115548>.
- [16]. Hassan, A., Baraghith, A.T., Atta, A.M. and El-Shafiey, T.F., 2021. Retrofitting of shear-damaged RC T-beams using U-shaped SHCC jacket. *Eng. Struct.*, 245, p.112892. <https://doi.org/10.1016/j.engstruct.2021.112892>.
- [17]. Afefy, H.M., Baraghith, A.T., Hassan, A. and Abuzaid, M.K., 2021. Strengthening of shear-deficient RC beams using near surface embedded precast cement-based composite plates (PCBCPs). *Eng. Struct.*, 244, p.112765. <https://doi.org/10.1016/j.engstruct.2021.112765>.
- [18]. Pisani, M.A., 1999. Strengthening by means of external prestressing. *Journal of Bridge Engineering*, 4(2), pp.131-135. [https://doi.org/10.1061/\(asce\)1084-0702\(1999\)4:2\(131\)](https://doi.org/10.1061/(asce)1084-0702(1999)4:2(131)).
- [19]. Adhikary, B.B. and Mutsuyoshi, H., 2006. Shear strengthening of reinforced concrete beams using various techniques. *Construction and building materials*, 20(6), pp.366-373. <https://doi.org/10.1016/j.conbuildmat.2005.01.024>.
- [20]. Colajanni, P., Recupero, A. and Spinella, N., 2017. Increasing the shear capacity of reinforced concrete beams using pretensioned stainless steel ribbons. *Structural Concrete*, 18(3), pp.444-453. <https://doi.org/10.1002/suco.201600089>.
- [21]. Ojaimi, M.F., 2021. Experimental Study on Shear Strengthening of Reinforced Concrete Beams Using Different Techniques of Concrete Jacketing. *Basrah Journal for Engineering Science*, 21(2). <http://dx.doi.org/10.33971/bjes.21.2.8>.
- [22]. Barnes, R.A., Baglin, P.S., Mays, G.C. and Subedi, N.K., 2001. External steel plate systems for the shear strengthening of reinforced concrete beams. *Engineering structures*, 23(9), pp.1162-1176. [https://doi.org/10.1016/s0141-0296\(00\)00124-3](https://doi.org/10.1016/s0141-0296(00)00124-3).
- [23]. Adhikary, B.B. and Mutsuyoshi, H., 2006. Shear strengthening of RC beams with web-bonded continuous steel plates. *Construction and Building Materials*, 20(5), pp.296-307. <https://doi.org/10.1016/j.conbuildmat.2005.01.026>.
- [24]. Adhikary, B.B., Mutsuyoshi, H. and Sano, M., 2000. Shear strengthening of reinforced concrete beams using steel plates bonded on beam web: experiments and analysis. *Construction and Building materials*, 14(5), pp.237-244. [https://doi.org/10.1016/s0950-0618\(00\)00023-4](https://doi.org/10.1016/s0950-0618(00)00023-4).
- [25]. Nguyen-Minh, L., Vo-Le, D., Tran-Thanh, D., Pham, T.M., Ho-Huu, C. and Rovňák, M., 2018. Shear capacity of unbonded post-tensioned concrete T-beams strengthened with CFRP and GFRP U-wraps. *Composite Structures*, 184, pp.1011-1029. <https://doi.org/10.1016/j.compstruct.2017.10.072>.
- [26]. Dias, S.J., Barros, J.A. and Janwaen, W., 2018. Behavior of RC beams flexurally strengthened with NSM CFRP laminates. *Composite Structures*, 201, pp.363-376. <https://doi.org/10.1016/j.compstruct.2018.05.126>.
- [27]. Ibrahim, M., Wakjira, T. and Ebead, U., 2020. Shear strengthening of reinforced concrete deep beams using near-surface mounted hybrid carbon/glass fibre reinforced polymer strips. *Engineering Structures*, 210, p.110412. <https://doi.org/10.1016/j.engstruct.2020.110412>.
- [28]. Khalifa, A. and Nanni, A., 2002. Rehabilitation of rectangular simply supported RC beams with shear deficiencies using CFRP composites. *Construction and building materials*, 16(3), pp.135-146. [https://doi.org/10.1016/S0950-0618\(02\)00002-8](https://doi.org/10.1016/S0950-0618(02)00002-8).
- [29]. Nanni, A., Ludovico, M.D. and Parretti, R., 2004. Shear strengthening of a PC bridge girder with NSM CFRP rectangular bars. *Advances in Structural Engineering*, 7(4), pp.297-309. <https://doi.org/10.1260/1369433041653570>.
- [30]. Ebead, U. and Saeed, H., 2013. Hybrid shear strengthening system for reinforced concrete beams: An experimental study. *Engineering Structures*, 49, pp.421-433. <https://doi.org/10.1016/j.engstruct.2012.11.039>.
- [31]. Mari, A., Cladera, A., Oller, E. and Bairan, J., 2014. Shear design of FRP reinforced concrete beams without transverse reinforcement. *Composites Part B: Engineering*, 57, pp.228-241. <https://doi.org/10.1016/j.compositesb.2013.10.005>.
- [32]. Khalifa, A., Gold, W.J., Nanni, A. and MI, A.A., 1998. Contribution of externally bonded FRP to shear capacity of RC flexural members. *Journal of composites for construction*, 2(4), pp.195-202. [https://doi.org/10.1061/\(asce\)1090-0268\(1998\)2:4\(195\)](https://doi.org/10.1061/(asce)1090-0268(1998)2:4(195)).
- [33]. Chaallal, O., Nollet, M.J. and Perraton, D., 1998. Shear strengthening of RC beams by externally bonded side CFRP strips. *Journal of composites for construction*, 2(2), pp.111-113. [https://doi.org/10.1061/\(asce\)1090-0268\(1998\)2:2\(111\)](https://doi.org/10.1061/(asce)1090-0268(1998)2:2(111)).
- [34]. Li, A., Diagana, C. and Delmas, Y., 2001. CRFP contribution to shear capacity of strengthened RC beams. *Engineering Structures*, 23(10), pp.1212-1220. [https://doi.org/10.1016/s0141-0296\(01\)00035-9](https://doi.org/10.1016/s0141-0296(01)00035-9).
- [35]. Boushelham, A. and Chaallal, O., 2008. Mechanisms of shear resistance of concrete beams strengthened in shear with externally bonded FRP. *Journal of Composites for Construction*, 12(5), pp.499-512. [https://doi.org/10.1061/\(asce\)1090-0268\(2008\)12:5\(499\)](https://doi.org/10.1061/(asce)1090-0268(2008)12:5(499)).
- [36]. Zhang, Z., Hsu, C.T.T. and Moren, J., 2004. Shear strengthening of reinforced concrete deep beams using carbon fiber reinforced polymer laminates. *Journal of Composites for Construction*, 8(5), pp.403-414. <https://doi.org/10.14359/5687>.
- [37]. De Lorenzis, L. and Teng, J.G., 2007. Near-surface mounted FRP reinforcement: An emerging technique for strengthening structures. *Composites Part B: Engineering*, 38(2), pp.119-143. <https://doi.org/10.1016/j.compositesb.2006.08.003>.
- [38]. Ali, H., Assih, J. and Li, A., 2021. Flexural capacity of continuous reinforced concrete beams strengthened or repaired by CFRP/GFRP sheets. *International Journal of Adhesion and Adhesives*, 104, p.102759. <https://doi.org/10.1016/j.ijadhadh.2020.102759>.
- [39]. Chen, G.M., Teng, J.G. and Chen, J.F., 2012. Process of debonding in RC beams shear-strengthened with FRP U-strips or side strips. *International Journal of Solids and Structures*, 49(10), pp.1266-1282. <https://doi.org/10.1016/j.ijsolstr.2012.02.007>.
- [40]. Koutas, L. and Triantafillou, T.C., 2013. Use of anchors in shear strengthening of reinforced concrete T-beams with FRP. *Journal of Composites for Construction*, 17(1), pp.101-107. [https://doi.org/10.1061/\(asce\)cc.1943-5614.0000316](https://doi.org/10.1061/(asce)cc.1943-5614.0000316).
- [41]. Mofidi, A., Chaallal, O., Benmokrane, B. and Neale, K., 2012. Performance of end-anchorage systems for RC beams strengthened in shear with epoxy-bonded FRP. *Journal of Composites for Construction*, 16(3), pp.322-331. [https://doi.org/10.1061/\(asce\)cc.1943-5614.0000263](https://doi.org/10.1061/(asce)cc.1943-5614.0000263).

- [42]. Bae, S.W. and Belarbi, A., 2013. Behavior of various anchorage systems used for shear strengthening of concrete structures with externally bonded FRP sheets. *Journal of Bridge Engineering*, 18(9), pp.837-8475592.0000420.
- [43]. Ceroni, F., Pecce, M., Matthys, S. and Taerwe, L., 2008. Debonding strength and anchorage devices for reinforced concrete elements strengthened with FRP sheets. *Composites Part B: Engineering*, 39(3), pp.429-441. <https://doi.org/10.1016/j.compositesb.2007.05.002>.
- [44]. Seo, S.Y., Feo, L. and Hui, D., 2013. Bond strength of near surface-mounted FRP plate for retrofit of concrete structures. *Composite Structures*, 95, pp.719-727. <http://dx.doi.org/10.1016/j.compstruct.2012.08.038>.
- [45]. Dias, S.J. and Barros, J.A., 2013. Shear strengthening of RC beams with NSM CFRP laminates: Experimental research and analytical formulation. *Composite Structures*, 99, pp.477-490. <https://doi.org/10.1016/j.compstruct.2012.09.026>.
- [46]. Bilotta, A., Ceroni, F., Nigro, E. and Pecce, M., 2015. Efficiency of CFRP NSM strips and EBR plates for flexural strengthening of RC beams and loading pattern influence. *Composite Structures*, 124, pp.163-175. <https://doi.org/10.1016/j.compstruct.2014.12.046>.
- [47]. Triantafyllou, G.G., Rousakis, T.C. and Karabinis, A.I., 2018. Effect of patch repair and strengthening with EBR and NSM CFRP laminates for RC beams with low, medium and heavy corrosion. *Composites Part B: Engineering*, 133, pp.101-111. <https://doi.org/10.1016/j.compositesb.2017.09.029>.
- [48]. Kuntal, V.S., Chellapandian, M. and Prakash, S.S., 2017. Efficient near surface mounted CFRP shear strengthening of high strength prestressed concrete beams—An experimental study. *Composite Structures*, 180, pp.16-28. <https://doi.org/10.1016/j.compstruct.2017.07.095>.
- [49]. Abdallah, M., Al Mahmoud, F., Khalil, N. and Khelil, A., 2023. Effect of the strengthening patterns on the flexural performance of RC continuous beams using FRP reinforcements. *Engineering Structures*, 280, p.115657. <https://doi.org/10.1016/j.engstruct.2023.115657>.
- [50]. Breveglieri, M., Aprile, A. and Barros, J.A., 2014. Shear strengthening of reinforced concrete beams strengthened using embedded through section steel bars. *Engineering structures*, 81, pp.76-87. <https://doi.org/10.1016/j.engstruct.2014.09.026>.
- [51]. Mofidi, A. and Chaallal, O., 2011. Shear strengthening of RC beams with EB FRP: Influencing factors and conceptual debonding model. *Journal of Composites for Construction*, 15(1), pp.62-74. [https://doi.org/10.1061/\(asce\)cc.1943-5614.0000153](https://doi.org/10.1061/(asce)cc.1943-5614.0000153).
- [52]. Mofidi, A., Chaallal, O., Benmokrane, B. and Neale, K., 2012. Experimental tests and design model for RC beams strengthened in shear using the embedded through-section FRP method. *Journal of Composites for Construction*, 16(5), pp.540-550. [https://doi.org/10.1061/\(asce\)cc.1943-5614.0000292](https://doi.org/10.1061/(asce)cc.1943-5614.0000292).
- [53]. Chaallal, O., Mofidi, A., Benmokrane, B. and Neale, K., 2011. Embedded through-section FRP rod method for shear strengthening of RC beams: Performance and comparison with existing techniques. *Journal of composites for construction*, 15(3), pp.374-383. [https://doi.org/10.1061/\(asce\)cc.1943-5614.0000174](https://doi.org/10.1061/(asce)cc.1943-5614.0000174).
- [54]. Van Hong Bui, L., Stitmannathum, B. and Ueda, T., 2020. Experimental investigation of concrete beams strengthened with embedded through-section steel and FRP bars. *Journal of Composites for Construction*, 24(5), p.04020052. [https://doi.org/10.1061/\(asce\)cc.1943-5614.0001055](https://doi.org/10.1061/(asce)cc.1943-5614.0001055).
- [55]. Fiset, M., Bastien, J. and Mitchell, D., 2023. Shear design of RC members strengthened with steel reinforcing bars embedded through section. *Engineering Structures*, 285, p.116050. <https://doi.org/10.1016/j.engstruct.2023.116050>.
- [56]. Breveglieri, M., Aprile, A. and Barros, J.A., 2015. Embedded Through-Section shear strengthening technique using steel and CFRP bars in RC beams of different percentage of existing stirrups. *Composite Structures*, 126, pp.101-113. <https://doi.org/10.1016/j.compstruct.2015.02.025>.
- [57]. Breveglieri, M., Aprile, A. and Barros, J.A., 2016. RC beams strengthened in shear using the Embedded Through-Section technique: Experimental results and analytical formulation. *Composites Part B: Engineering*, 89, pp.266-281. <https://doi.org/10.1016/j.compositesb.2015.11.023>.
- [58]. Moradi, E., Naderpour, H. and Kheyroddin, A., 2020. An experimental approach for shear strengthening of RC beams using a proposed technique by embedded through-section FRP sheets. *Composite Structures*, 238, p.111988. <https://doi.org/10.1016/j.compstruct.2020.111988>.
- [59]. Bianco, V., Barros, J.A. and Monti, G., 2009. Bond model of NSM-FRP strips in the context of the shear strengthening of RC beams. *Journal of Structural Engineering*, 135(6), pp.619-631. [http://dx.doi.org/10.1061/\(ASCE\)0733-9445\(2009\)135:6\(619\)](http://dx.doi.org/10.1061/(ASCE)0733-9445(2009)135:6(619)).
- [60]. Ali, M.M., Oehlers, D.J., Griffith, M.C. and Seracino, R., 2008. Interfacial stress transfer of near surface-mounted FRP-to-concrete joints. *Engineering structures*, 30(7), pp.1861-1868. <http://dx.doi.org/10.1016/j.engstruct.2007.12.006>.
- [61]. Yuan, H., Teng, J.G., Seracino, R., Wu, Z.S. and Yao, J., 2004. Full-range behavior of FRP-to-concrete bonded joints. *Engineering structures*, 26(5), pp.553-565. <http://dx.doi.org/10.1016/j.engstruct.2003.11.006>.
- [62]. ACI Committee, 2019. Building code requirements for structural concrete (ACI 318-19) and commentary. American Concrete Institute, Farmington Hills, MI, 519 ppfv.
- [63]. ASTM C39/C39M-21, Standard Test Method for Compressive Strength of Cylindrical Concrete Specimens, ASTM International, 2021. www.astm.org.
- [64]. ASTM A615/A615M-16, "Standard specification for deformed and plain carbon steel bars for concrete reinforcement." ASTM International, 2016. www.astm.org.
- [65]. ACI Committee 440.2R-17, 2017. Guide for the Design and Construction of Externally Bonded FRP Systems for Strengthening Concrete Structures. Sika. <https://egy.sika.com>.
- [66]. Khalil, A.E., Etman, E., Atta, A., Baraghith, A. and Behiry, R., 2019. The Effective Width in Shear Design of Wide-shallow Beams: A Comparative Study. *KSCE Journal of Civil Engineering*, 23(4), pp.1670-1681. <https://doi.org/10.1007/s12205-019-0830-7>.
- [67]. Dias, S.J.E. and Barros, J.A.O., 2011. Shear strengthening of RC T-section beams with low strength concrete using NSM CFRP laminates. *Cement and Concrete Composites*, 33(2), pp.334-345. <http://dx.doi.org/10.1016/j.cemconcomp.2010.10.002>.
- [68]. Dias, S.J. and Barros, J.A., 2010. Performance of reinforced concrete T beams strengthened in shear with NSM CFRP laminates. *Engineering Structures*, 32(2), pp.373-384. <http://dx.doi.org/10.1016/j.engstruct.2009.10.001>.
- [69]. Rizzo, A. and De Lorenzis, L., 2009. Behavior and capacity of RC beams strengthened in shear with NSM FRP reinforcement. *Construction and Building Materials*, 23(4), pp.1555-1567. <http://dx.doi.org/10.1016/j.conbuildmat.2007.08.014>.
- [70]. Afefy, H.M., Baraghith, A.T. and Mahmoud, M.H., 2020. Retrofitting of defected reinforced-concrete cantilever slabs using different techniques. *Magazine of Concrete Research*, 72(14), pp.703-719. <https://doi.org/10.1680/jmacr.18.00340>.
- [71]. Behiry, R.N. and El Korany, T.M., 2023. Strain-hardening cementitious composites versus normal mortar for shear strengthening of concrete beams. *IOSR Journal of Mechanical and Civil Engineering (IOSR-JMCE)*, 20(2), pp. 61-75. <http://dx.doi.org/10.9790/1684-2002026175>.